Electronic supplementary information

Rational functionalization of reduced graphene oxide with imidazole group for the electrochemical sensing of bisphenol A–an endocrine disruptor

Bhaskar Manna*

Functional Materials and Electrochemistry Laboratory, Department of Chemistry,

Indian Institute of Technology Kharagpur,

Kharagpur 721302, West Bengal, India

*Corresponding author.

E-mail: bhaskar_manna@chem.iitkgp.ernet.in;

bhasmanna.chem@yahoo.com

Synthesis of graphene oxide (GO)

GO was synthesized from pristine graphite according to modified Hummers method. Briefly 25 mL of concentrated H_2SO_4 was slowly poured into a mixture of graphite powder (0.5 g) and $NaNO_3$ (0.5 g) in a 500 mL round bottom (RB) flask at 0 °C. Solid $KMnO_4$ (3 g) was added to the RB at < 5 °C and the mixture was stirred for 1 h at room temperature. Water (150 mL) was slowly added to the RB and stirred for another 15 min. Then H_2O_2 solution (30%) was added to the RB until the gas evolution was ceased. The residue was then washed repeatedly with 15% HCl solution till the washing solution gave negative test for sulfate ion (tested with $BaCl_2$ solution). After that the residue was repeatedly washed with Millipore water and dried in vacuum to get the yellow-brown solid GO.

Figure S1

Electrochemical reduction of GO-Hist. The potential of GO-Hist electrode was cycled within the potential window 0 to -0.8 V (20 cycles) at a sweep rate of 50 mV s^{-1}.

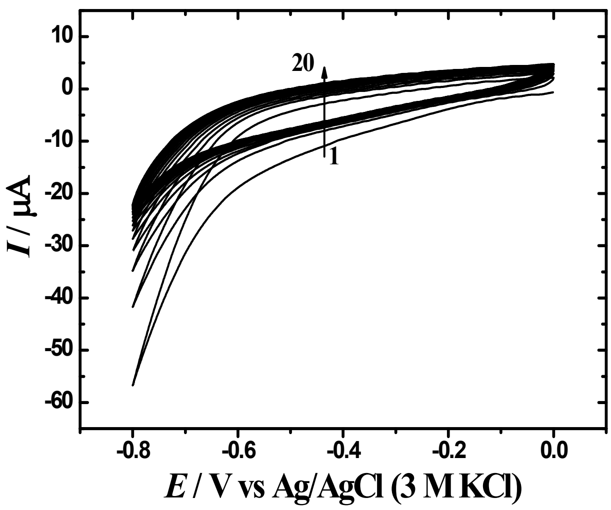

Figure S2

Raman spectral profiles of GO, GO-Hist, rGO and rGO-Hist.

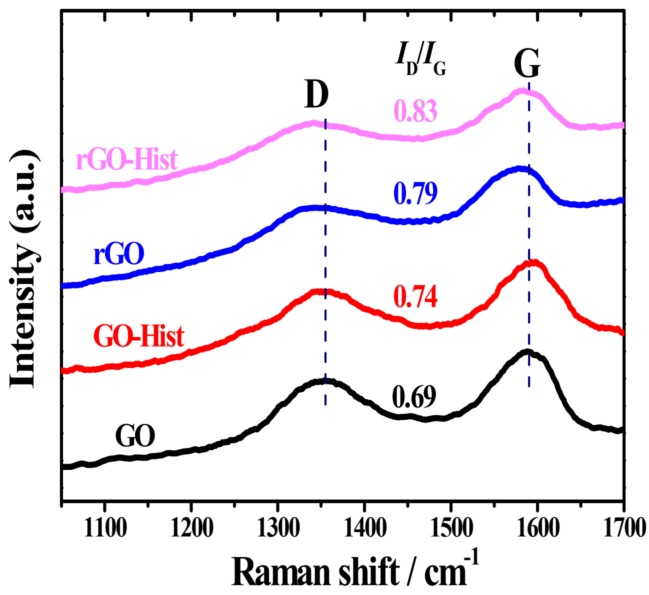

Figure S3

TEM images of GO (A), GO-Hist (B) and rGO-Hist (C). EDX analysis of GO (D), GO-Hist (E) and rGO-Hist (F).

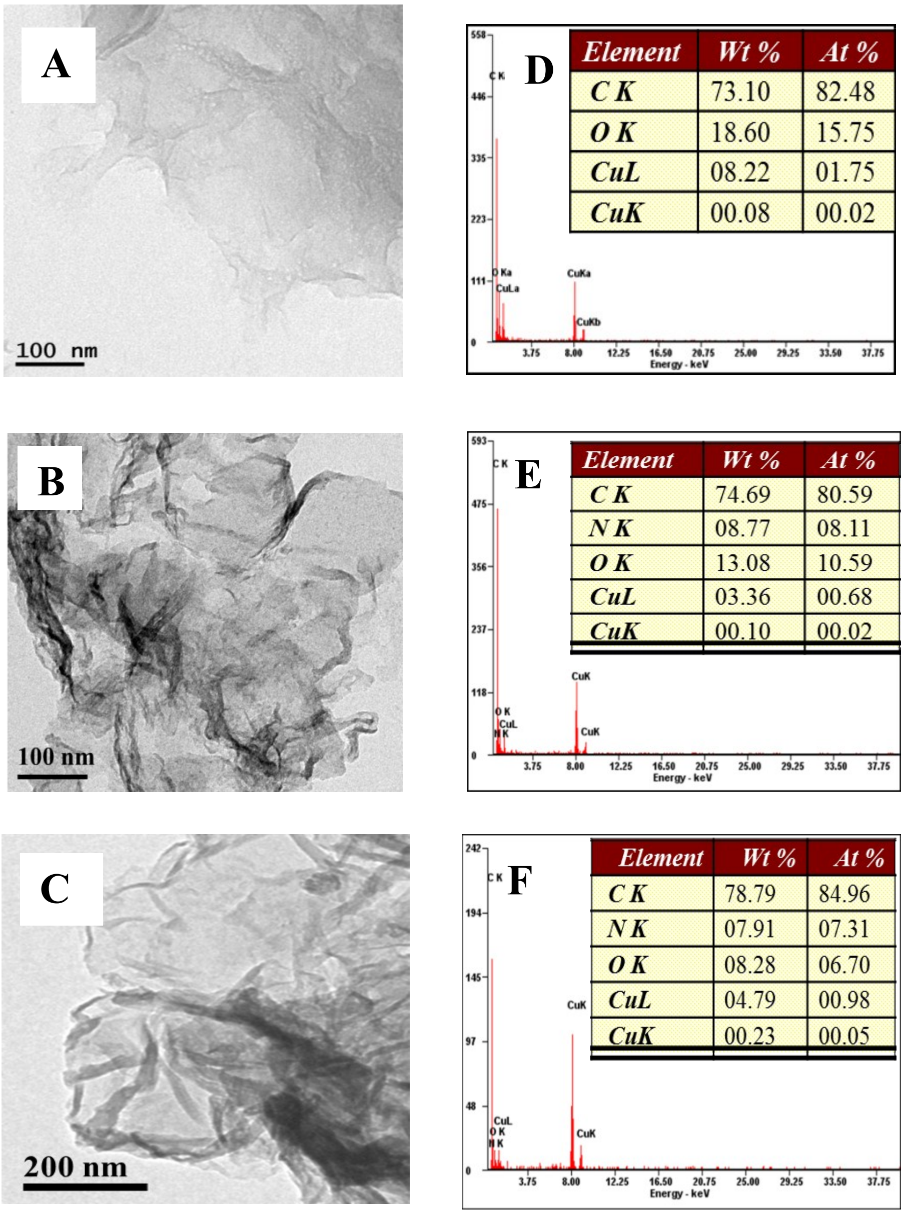

Figure S4

Survey scan (A) and deconvoluted (B) C1s XPS profiles of GO

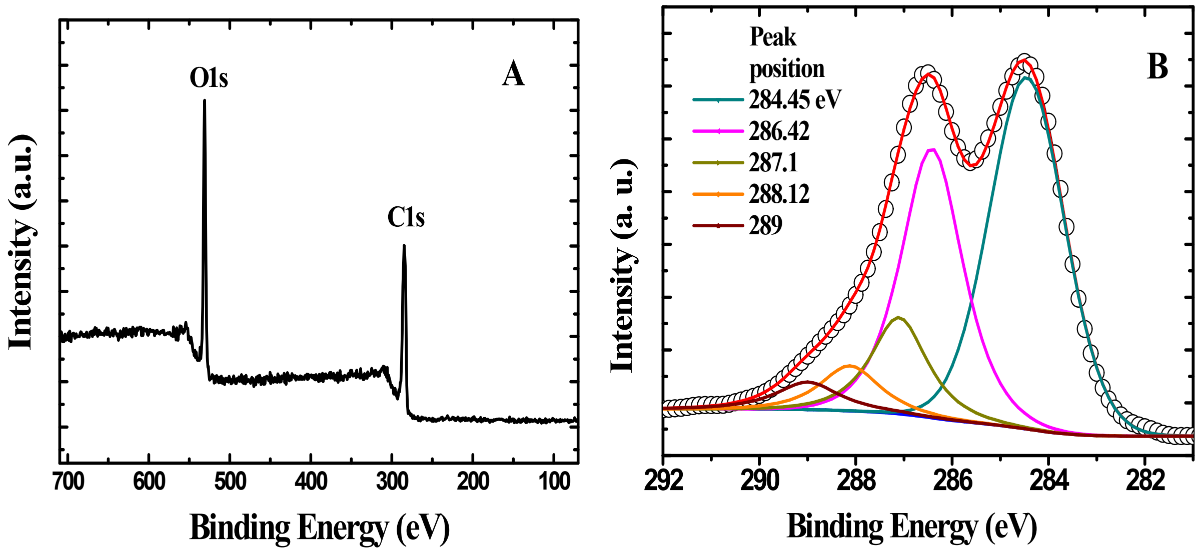

Figure S5

(A) Cyclic voltamograms of rGO-Hist modified electrode in 0.1 M PBS (pH 7.2) at different scan rates: (a) 25, (b) 50, (c) 75, (d) 100, (e) 150 mV s^{-1} containing 20 μM BPA. **(B)** Plot of peak current (i_p) vs (scan rate)$^{1/2}$.

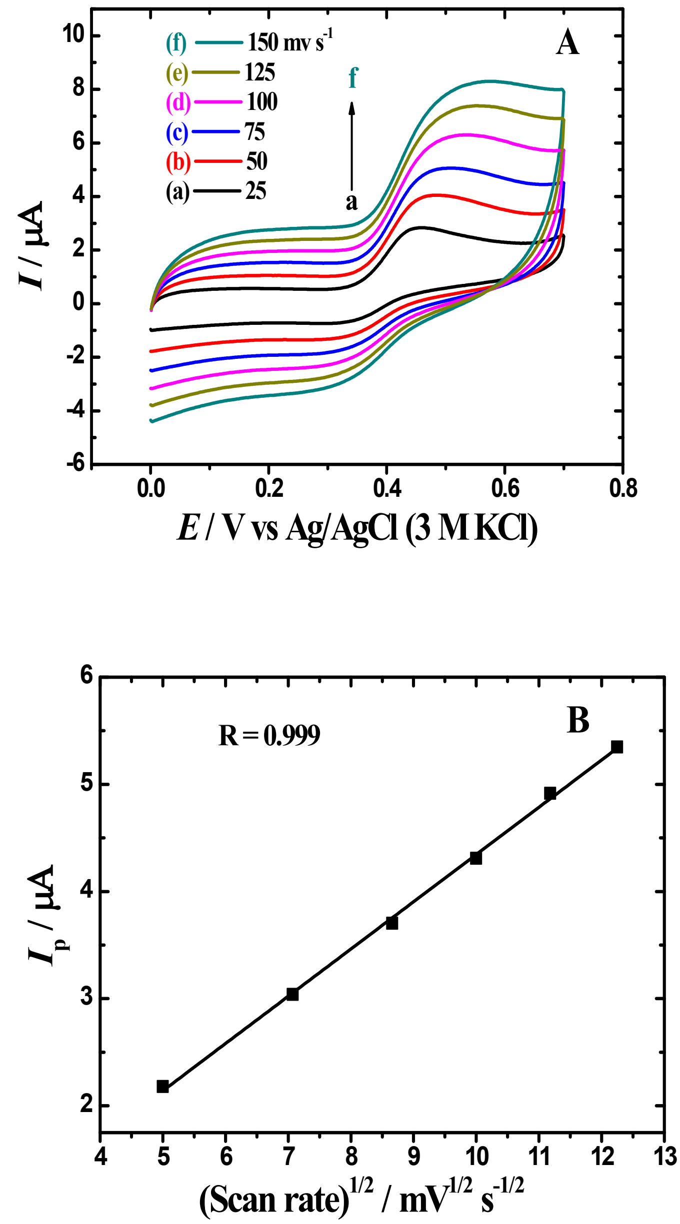

Figure S6

Amperometric i–t curves for the oxidation of BPA at GO, GO-Hist, rGO and rGO-Hist electrodes in a stirred solution of 0.1 M PBS (pH 7.2). Each addition increased the concentration of BPA by 5 μM.

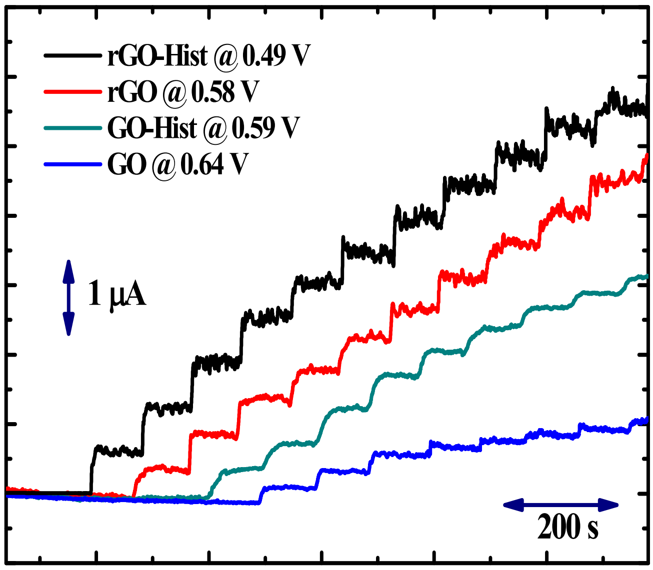

Figure S7

Amperometric response depicting the detection of low concentration of BPA in 0.1 M PBS of pH 7.2 polarizing the rGO-Hist electrode at 0.49 V.

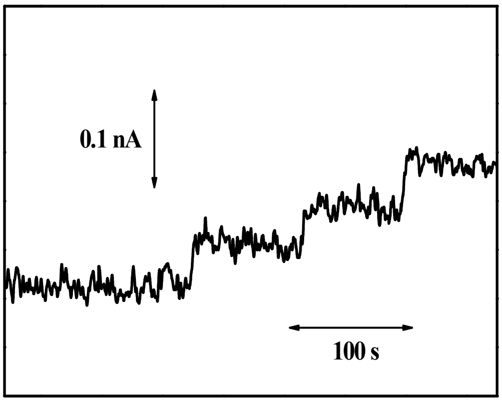

Figure S8

Amperometric i-t curve illustrating the operational stability of the rGO-Hist electrode towards BPA measurement in 0.1 M PBS of pH 7.2. The electrode was polarised at 0.49 V and 20 μM BPA was injected.

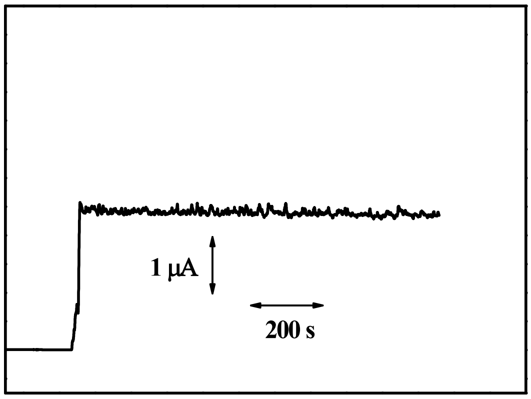

Figure S9

Amperometric i-t curve illustrating the interference effect of other analytes for the sensing of BPA at rGO-Hist electrode in 0.1 M PBS of pH 7.2. BPA, K^{+}, Zn^{2+}, Ca^{2+}, Mg^{2+}, Cu^{2+}, Fe^{3+}, Cl^{-}, Br^{-}, NH_4^{+}, SO_4^{2-}. CO_3^{2-}, NO_3^{-}, hydroquionone, catechol, 4-nitrophenol and nitrobenzene (20 µM each) were injected one after another as indicated. The electrode was polarised at 0.49 V.

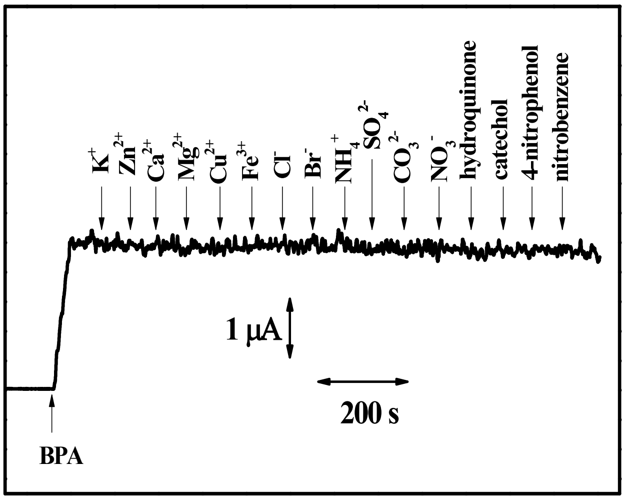

Table S1

Analytical performances of several electrochemical BPA sensor.

Sl. No.	Sensing Interface	Potential (V)	Linear range (nM)	Limit of Detection (LOD) (nM)	Reference	Remarks
1	Pt/GR-CNTs/GCE	0.65 vs SCE	60–80000	42	1	Linear range starts from high concentration and LOD is higher than this work
2	CTAB-CPE	0.87 vs SCE	25–1000	7.5	2	Short linear range, linear range starts from high concentration and LOD is higher than this work
3	Arg-G/GCE	0.511 vs SCE	5–40000	1.1	3	LOD is higher than this work
4	PAMAM-Fe_3O_4	0.541 vs SCE	10–3070	5	4	Short linear range and LOD is higher than this work
5	CoPc-CPE	0.454 vs SCE	87.5–12500	10	5	Short linear range, linear range starts from high concentration and LOD is higher than this work
6	AuNPs/SGNF/GCE	0.343 vs SCE	80–250000	35	6	Linear range starts from high concentration and LOD is higher than this work
7	Tyr-SF-MWNTs-CoPc/GCE	0.625 vs SCE	50–3000	30	7	Short linear range, linear range starts from high concentration and LOD is higher than this work
8	MWCNT-GNPs/GCE	–	20–20000	7.5	8	Short linear range, linear range starts from high concentration and LOD is higher than this work
9	3Au-1Pd alloy NPs/GN/GCE	0.528 vs Ag/ AgCl electrode	10–5000	4	9	Short linear range and LOD is higher than this work
10	CS-Fe_3O_4/GCE	0.541 vs SCE	50–30000	8	10	Linear range starts from high concentration and LOD is higher than this work
11	CNT/GCE	0.590 vs Ag/AgCl	300–100000	98	11	Linear range starts from high concentration and LOD is higher than this work

12	SWNT-tyrosinase/CPE	-0.15 vs Ag/AgCl	100–12000	20	12	Short linear range, linear range starts from high concentration and LOD is higher than this work
13	MCM-41/CPE	–	220–8800	38	13	Short linear range, linear range starts from high concentration and LOD is higher than this work
14	Boron-doped diamond electrode	0.9 vs Ag/AgCl (3 M KCl)	440–5200	210	14	Short linear range, linear range starts from high concentration and LOD is higher than this work
15	Tyr-NGP-Chi/GC	-0.1 vs Ag/AgCl (3 M KCl)	100–2000	33	15	Short linear range, linear range starts from high concentration and LOD is higher than this work
16	CS/MNPs-rGO/GCE	0.49 vs SCE	60–11000	17	16	Short linear range, linear range starts from high concentration and LOD is higher than this work
17	N-GS/GCE	0.54 vs SCE	10–1300	5	17	Short linear range and LOD is higher than this work
18	CNHs-Nafion/GCE	–	200000–1000000	1800	18	Linear range starts from high concentration and LOD is higher than this work
19	f-SWCNT/PC4/GCE	0.623 vs SCE	99–5794	32	19	Short linear range, linear range starts from high concentration and LOD is higher than this work
20	MWCNT/MAM/GCE	0.56 vs SCE	10–40800	5	20	LOD is higher than this work
21	Sol-gel MIP/MWCNTs-GNPs /Au	0.5 vs Ag/AgCl electrode	113–8210000	3.6	21	Linear range starts from high concentration and LOD is higher than this work
22	MWCNTs-PEI/GCE	0.5 vs SCE	10–50000	3.3	22	LOD is higher than this work
23	PEDOT/GCE	0.5 vs Ag/AgCl electrode	40000–410000	22000	23	Linear range starts from high concentration and LOD is higher than this work
24	f-MWCNTs/AuNPs nanocomposite/aptasensor	–	0.1–10	0.05	24	Short linear range and LOD is higher than this work
25	PGA/MWCNT-NH_2/GCE	–	100–10000	20	25	Short linear range, linear range starts from high concentration and LOD is higher than this work

26	GR-IL/GCE	0.48 vs Ag/AgCl electrode	20–2000	8	26	Short linear range, linear range starts from high concentration and LOD is higher than this work
27	LDH/GCE	0.454 vs SCE	10–1050	5	27	Short linear range and LOD is higher than this work
28	CTS-GR/CILE	0.436 vs SCE	100–800000	26.4	28	Linear range starts from high concentration and LOD is higher than this work
29	ELDH/GCE	0.489 vs SCE	20–1510	6.8	29	Short linear range, linear range starts from high concentration and LOD is higher than this work
30	GR/Au-Tyr-CS/GCE	0.47 vs SCE	2.5–3000	1	30	Short linear range and LOD is higher than this work
31	Tyr-rGO-DAPPT/GCE	0.1 vs SCE	1–38000	0.35	31	LOD is higher than this work
32	TiO_2/Au NTAs	0.53 vs Ag/AgCl electrode	100-38900 (with UV light) and 100-28900 (without UV light)	6.2 (with UV light) and 47 (without UV light)	32	Linear range starts from high concentration and LOD is higher than this work
33	SWCNT-CD/GCE	0.543 vs SCE	10.8–18500	1	33	Short linear range and LOD is higher than this work
34	Fe_3O_4-NPs-CB/GCE	0.542 vs SCE	0.1–50000	0.031	34	LOD is higher than this work
35	NGP/GCE	0.49 vs Ag/AgCl electrode	100–50000	12.1	35	Linear range starts from high concentration and LOD is higher than this work
36	rGO-Hist	0.49 vs Ag/AgCl (3 M KCl)	upto 30000	0.03	This work	Practically usable linear range and very low LOD

References

1 Z. Zheng, Y. Du, Z. Wang, Q. Feng and C. Wang, *Analyst*, 2013, **138**, 693–701.

2 W. Huang, Bull. *Korean Chem. Soc.*, 2005, **26**, 1560–1564.

3 Y. Zhang, L. Wang, D. Lu, X. Shi, C. Wang and X. Duan, *Electrochim. Acta*, 2012, **80**, 77–83.

4 H. Yin, L. Cui, Q. Chen, W. Shi, S. Ai, L. Zhu and L. Lu, *Food Chem.*, 2011, **125**, 1097–1103.

5 H. Yin, Y. Zhou and S. Ai, *J. Electroanal. Chem.*, 2009, **626**, 80–88.

6 X. Niu, W. Yang, G. Wang, J. Ren, H. Guo and J. Gao, *Electrochim. Acta*, 2013, **98**, 167–175.

7 H. Yin, Y. Zhou, J. Xu, S. Ai, L. Cui and L. Zhu, *Anal. Chim. Acta*, 2010, **659**, 144–150.

8 X. Tu, L. Yan, X. Luo, S. Luo and Q. Xie, *Electroanalysis*, 2009, **21**, 2491–2494.

9 C. Huang, Y. Wu, J. Chen, Z. Han, J. Wang, H. Pan and M. Du, *Electroanalysis*, 2012, **24**, 1416–1423.

10 C. Yu, L. Gou, X. Zhou, N. Bao and H. Gu, *Electrochim. Acta*, 2011, **56**, 9056–9063.

11 D. Vega, L. Agüí, A. Gonzalez-Cortés, P. Yáñez-Sedeño and J. M. Pingarron, *Talanta*, 2007, **71**, 1031–1038.

12 D. G. Mita, A. Attanasio, F. Arduini, N. Diano, V. Grano, U. Bencivenga, S. Rossi, A. Amine and D. Moscone, *Bisens. Bioelectron.*, 2007, **23**, 60–65.

13 F. Wang, J. Yang and K. Wu, *Anal. Chim. Acta*, 2009, **638**, 23–28.

14 G. F. Pereira, L. S. Andrade, R. C. Rocha-Filho, N. Bocchi and S. R. Biaggio, *Electrochim. Acta*, 2012, **82**, 3–8.

15 L. Wu, D. Deng, J. Jin, X. Lu and J. Chen, *Bisens. Bioelectron.*, 2012, **35**, 193–199.

16 Y. Zhang, Y. Cheng, Y. Zhou, B. Li, W. Gu, X. Shi and Y. Xian, *Talanta*, 2013, **107**, 211–218.

17 H. Fan, Y. Li, D. Wu, H. Ma, K. Mao, D. Fan, B. Du, H. Li and Q. Wei, *Anal. Chim. Acta*, 2012, **711**, 24–28.

18 G. Xu, L. Gong, H. Dai, X. Li, S. Zhang, S. Lu, Y. Lin, J. Chen, Y. Tong and G. Chen, *Anal. Methods*, 2013, **5**, 3328–3333.

19 L. Zhang, Y.-P. Wen, Y.-Y. Yao, Z.-F. Wang, X.-M. Duan and J.-K. Xu, *Chin. Chem. Lett.*, 2014, **25**, 517–522.

20 Y. Li, Y. Gao, Y. Cao and H. Li, *Sens. Actuators, B*, 2012, **171-172**, 726–733.

21 J. Huang, X. Zhang, Q. Lin, X. He, X. Xing, H. Huai, W. Lian and H. Zhu, *Food Control*, 2011, **22**, 786–791.

22 Y. Yang, H. Zhang, C. Huang and N. Jia, *Sens. Actuators, B*, 2016, **235**, 408–413.

23 E. Mazzotta, C. Malitesta and E. Margapoti, *Anal. Bioanal. Chem.*, 2013, **405**, 3587–3592.

24 B. Deiminiat, G. H. Rounaghi, M. H. Arbab-Zavar and I. Razavipanah, *Sens. Actuators, B*, 2017, **242**, 158–166.

25 Y. Lin, K. Liu, C. Liu, L. Yin, Q. Kang, L. Li and B. Li, *Electrochim. Acta*, 2014, **133**, 492–500.

26 P. Jing, X. Zhang, Z. Wu, L. Bao, Y. Xu, C. Liang and W. Cao, *Talanta*, 2015, **141**, 41–46.

27 H. Yin, L. Cui, S. Ai, H. Fan and L. Zhu, *Electrochim. Acta*, 2010, **55**, 603–610.

28 Q. Wang, Y. Wang, S. Liu, L. Wang, F. Gao, F. Gao and W. Sun, *Thin Solid Films*, 2012, **520**, 4459–4464.

29 T. Zhan, Y. Song, Z. Tan and W. Hou, *Sens. Actuators, B*, 2017, **238**, 962–971.

30 D. Pan, Y. Gu, H. Lan, Y. Sun and H. Gao, *Anal. Chim. Acta*, 2015, **853**, 297–302.

31 R. Li, Y. Wang, Y. Deng, G. Liu, X. Hou, Y. Huang and C. Li, *Electroanalysis*, 2016, **28**, 96–102.

32 L. Hu, C.-C. Fong, X. Zhang, L. L. Chan, P. K. S. Lam, P. K. Chu, K.-Y. Wong and M. Yang, *Environ. Sci. Technol.*, 2016, **50**, 4430–4438.

33 Y. Gao, Y. Cao, D. Yang, X. Luo, Y. Tang and H. Li, *J. Hazard. Mater.*, 2012, **199**, 111–118.

34 C. Hou, W. Tang, C. Zhang, Y. Wang and N. Zhu, *Electrochim. Acta*, 2014, **144**, 324–331.

35 X. Yan, C. Zhou, Y. Yan and Y. Zhu, *Electroanalysis*, 2015, **27**, 2718–2724.